TẠP CHÍ KHOA HỌC
Khoa học Tự nhiên và Công nghệ, Số 16 (6/2019) tr. 9 - 26

PHASE STRUCTURE OF BINARY ATOMIC BOSE-FERMI MIXTURE AT FINITE TEMPERATURE

Nguyen Tuan Anh[1], Đinh Thanh Tam[2]
[1] Electric Power University
[2]Tay Bac University

Abstract: *A variety of experimental realizations of binary atomic Bose-Fermi mixtures have brought opportunities for studying composite quantum systems with different spin-statistics. The binary atomic mixtures can exhibit a structural transition from a mixture into phase separation as the boson-fermion interaction increases. By using a Cornwall-Jackiw-Tomboulis formalism to evaluate the grand partition function and thermodynamic grand potential, we obtain the effective potential of binary Bose-Fermi mixtures. Thermodynamic quantities in a broad range of temperatures and interactions are also derived. The structural transition can be identified as a loop of the effective potential curve, and the volume fraction of phase separation can be determined by the lever rule. For* $^{40}\mathrm{K}-^{87}\mathrm{Rb}$ *and* $^{6}\mathrm{Li}-^{87}\mathrm{Rb}$ *mixtures, we present the phase diagrams of the mixtures at zero and finite temperatures.*

PACS number: 03.75.Mn, 05.30.Jp, 05.70.Fh, 05.70.Jk, 67.85.Hj, 67.85.Fg.

1. Introduction

After the successful experiments [1]-[7] a lot of new interesting phenomena of ultracold quantum gases have been discovered, both theoretically and experimentally, providing an attractive way to study many-body systems of atoms with short-range interactions. Owing to the technique of sympathetic cooling, Fermi gases to be cold efficiently by mixing them with bosons [8]. Hence, this has stimulated the investigation of Bose-Fermi mixtures.

On the experimental side, after Bose-Einstein condensation (BEC) in ultracold atoms was observed, further developments to mix ultracold bosons and fermions with different spin-statistics have made. For example, binary atomic ^{6}Li and ^{7}Li mixtures was achieved in 2001 [9-10]. Then, other binary atomic Bose-Fermi mixtures have been produced, including ^{40}K and ^{87}Rb [11], ^{6}Li and ^{87}Rb [12], ^{84}Sr and ^{87}Sr [13], ^{6}Li and ^{41}K [14] [15], ^{6}Li and ^{133}Cs [16], etc.

On the theoretical side, Bose-Fermi mixtures are of interest already at the mean-field level. Depending on the density of fermions and the value of the Bose-Fermi and Bose-Bose scattering lengths, a structural transition into phase separation is exhibited if the Bose-Fermi repulsion is too strong [17]. In turn, for sufficiently strong attractive interactions, the mixture is

Ngày nhận bài: 23/01/2019. Ngày nhận đăng: 26/02/2019.
Liên lạc: Đinh Thanh Tâm, e-mail: tamdt@utb.edu.vn

unstable. Signatures for a collapse have been observed experimentally [18]-[20] in the situation of the attractive Bose-Fermi interactions applied to the case of ^{40}K-^{87}Rb mixtures. The control of the Bose-Fermi scattering length using magnetically tunable Feshbach resonances [21] opens the possibility to explore novel phases in Bose-Fermi mixtures with nontrivial many-body correlations.

One interesting property of the binary atomic Bose-Fermi mixture is that at low temperatures, the bosons form BEC in a broken-symmetry phase while the fermions are in a normal, symmetric phase. The BEC transition adds additional features and challenges to the study of stable structures of Bose-Fermi mixtures.

Continuing on the development of previous studies on the phase structures of BEC and binary BECs [22], [23], in this paper, we implement a theoretical framework capable of describing both bosons and fermions in a broad range of temperature and interactions to investigate the properties and phase structure of binary atomic Bose-Fermi mixtures. The framework is based on the effective action method for composite systems named as Cornwall-Jackiw-Tombolis (CJT) formalism from quantum field theory [24-25], which has been applied successfully to bosons [22-27] and fermions [28-29], respectively.

We remark that atomic Bose-Fermi superfluid-superfluid mixtures have also been studied further [30-31], in which, adding components of bosons, superfluids of fermions require two components to form the Cooper pairs, then the mixture requires at least three components of atoms. Here we focus only on binary boson-fermion mixtures, the theoretical framework will be generalized to superfluid mixtures based on the effective action method in the next paper. The effective action method for composite systems have given relevant studies, especially on phase transitions, of boson-boson mixtures (known as the binary Bose gases) [23], [32] and fermion-fermion mixtures [33], [34]. However, the different spin-statistics make binary Bose-Fermi mixtures particularly interesting and challenging.

Let us start from the following Lagrangian of a mixture of bosonic (b) and fermionic (f) atoms (in $\hbar = 1$ units):

$$\pounds = \phi^* \left(-i\frac{\partial}{\partial t} - \frac{\nabla^2}{2m_b} \right) \phi + \psi^* \left(-i\frac{\partial}{\partial t} - \frac{\nabla^2}{2m_f} \right) \psi - V(\phi, \psi) \qquad (1)$$

$$V(\phi, \psi) = \mu_b \phi^* \phi + \mu_f \psi^* \psi - \frac{\lambda_b}{2} (\phi^* \phi)^2 - \lambda_f \psi^*_\uparrow \psi^*_\downarrow \psi_\downarrow \psi_\uparrow - \frac{\lambda_{bf}}{2} (\phi^* \phi)(\psi^* \psi),$$

where $\psi = \{\psi_\uparrow, \psi_\downarrow\}$, μ_b, (μ_f) is chemical potential ϕ, (ψ); m_b, (m_f) - the mass of atomic Boson and Fermion; λ_b, λ_f, λ_{bf} are the coupling constants:

$\lambda_i = 4\pi\hbar^2 a_i / m_i$, $i = b, f$; a_i are wave scattering lengths corresponding to collisions between atoms of the same type, a_{bf} is wave scattering length corresponding to collision between the other type; $\lambda_{bf} = 4\pi\hbar^2 a_{bf} / m_{bf}$, with $m_{bf} = m_b m_f / (m_b + m_f)$ reduced mass.

Lagrangian (1) does change when replace the operator filed ϕ by $e^{i\alpha}\phi$ and ψ by $e^{i\beta}\psi$. That means Lagrangian is invariant with respect to transformation phase of the symmetric group Unita U(1) $\times$ U(1). Hence, if Lagrangian is broken spontaneous symmetry to U(1) $\times$ U(1) group, then two Boson Goldstone are produced according to the Goldstone theorem.

We use hereafter the imaginary time formalism of Matsubara and work in Euclidean space-time. The Feynman rules are the same as those at zero temperature, except that

$$\int \frac{d^4k}{(2\pi)^4} f(k) \to \frac{1}{\beta}\sum_n \int \frac{d^3k}{(2\pi)^3} f(\omega_n, \vec{k}) \equiv \int_\beta f(k),$$

where $\omega_n = 2\pi n/\beta$ for boson, $\omega_n = \pi(2n+1)/\beta$ for fermion, $\beta = 1/T$.

In this work we show the results of ^{40}K-^{87}Rb and ^{6}Li-^{87}Rb mixtures, but the framework should be applicable to other binary Bose-Fermi mixtures as well.

The paper is organized as follows. Section 2 outlines the CJT approach of binary atomic Bose-Fermi mixtures. It shows how to construct the thermodynamic potential, energy, pressure and the thermodynamic quantities. Section 3 shows how to identify phase structures from the self-consistent equations of bosons and fermions. The phase diagrams and BEC for selected parameters at zero and finite temperatures are presented. Typical density profiles of the condensates are also presented. Finally, Section 4 concludes our work. The Appendix summarizes the integrals and approximations.

2. The CJT formalism and Goldstone restoration

Assumed that the expectation of boson field has a non-zero value ϕ_0, and there is a fermion pairing. Thus, by shifting

$$\phi \to \phi_0 + \tilde{\phi} = \phi_0 + \frac{1}{\sqrt{2}}(\phi_1 + i\phi_2) \tag{2}$$

$$\lambda_f \psi^*_\uparrow \psi_\uparrow \psi^*_\downarrow \psi_\downarrow \to \lambda_f \psi^*_\uparrow \psi_\uparrow \psi^*_\downarrow \psi_\downarrow - \psi_\uparrow \Delta^* \psi_\downarrow - \psi^*_\uparrow \Delta \psi^*_\downarrow + \frac{1}{\lambda_f}\Delta^*\Delta \tag{3}$$

we have a new Lagrangian

$$\pounds = \frac{i}{2}\Phi D_0^{-1}\Phi + \Psi G_0^{-1}\Psi - \mu_b\phi_0^2 + \frac{\lambda_b}{2}\phi_0^4 + \frac{1}{\lambda_f}\Delta^*\Delta + \frac{\lambda_b}{2}\sqrt{2}\phi_0\phi_1(\phi_1^2+\phi_2^2) + \frac{\lambda_b}{8}(\phi_1^2+\phi_2^2)^2$$

$$- \lambda_f \psi^*_\uparrow \psi_\uparrow \psi_\downarrow \psi^*_\downarrow + \frac{\lambda_{bf}}{2}\sqrt{2}\phi_0\phi_1(\psi^*_\uparrow\psi_\uparrow + \psi^*_\downarrow\psi_\downarrow) + \frac{\lambda_{bf}}{4}(\phi_1^2+\phi_2^2)(\psi^*_\uparrow\psi_\uparrow - \psi_\downarrow\psi^*_\downarrow) \tag{4}$$

where we put $\Phi = \begin{pmatrix}\phi_1\\ \phi_2\end{pmatrix}$ and $\Psi = \begin{pmatrix}\psi_\uparrow\\ \psi^*_\downarrow\end{pmatrix}$, the tree-level propagators in momentum space are

$$D_0^{-1}=\begin{pmatrix} \frac{\vec{k}^2}{2m_b}+M_{\phi_1} & -\omega_b \\ \omega_b & \frac{\vec{k}^2}{2m_b}+M_{\phi_2} \end{pmatrix}\omega_b = 2n\pi T; \qquad (5)$$

$$G_0^{-1}=\begin{pmatrix} -i\omega_f+\frac{\vec{k}^2}{2m_f}+M_\psi & -\Delta \\ -\Delta^* & -i\omega_f-\frac{\vec{k}^2}{2m_f}-M_\psi \end{pmatrix}\omega_f=(2n+1)\pi T. \qquad (6)$$

with

$$\tilde{\mu}_{b_1} = -\mu_b+3\lambda_b\phi_0^2\tilde{\mu}_{b_2} = -\mu_b+\lambda_b\phi_0^2\tilde{\mu}_f = -\mu_f+\frac{\lambda_{bf}}{2}\phi_0^2$$

Hence

$$\det D_0^{-1}=0\rightarrow E_\phi^2=\left(\frac{\vec{k}^2}{2m_b}\tilde{\mu}_{b_1}\right)\left(\frac{\vec{k}^2}{2m_b}+\tilde{\mu}_{b_2}\right) \qquad (7)$$

$$\det G_0^{-1}=0\rightarrow E_\psi^2=\left(\frac{\vec{k}^2}{2m_f}+\tilde{\mu}_f\right)^2+\Delta^*\Delta \qquad (8)$$

In tree-level approximation, $U=-\pounds_0$ we have

$$\frac{\delta U}{\delta\phi_0}=0\rightarrow -\mu_b\phi_0+\lambda_b\phi_0^3=0$$

$$\frac{\delta U}{\delta\Delta}=0\rightarrow \Delta^*=0$$

$$\frac{\delta U}{\delta\Delta^*}=0\rightarrow \Delta=0 \qquad (9)$$

Inserting (9) into (7) and (8), it provides

$$E_b^2=\left(\frac{\vec{k}^2}{2m_b}+2\lambda_b\phi_0^2\right)\frac{\vec{k}^2}{2m_b}\Rightarrow E_b=\pm\sqrt{\left(\frac{\vec{k}^2}{2m_b}+2\lambda_b\phi_0^2\right)\frac{\vec{k}^2}{2m_b}} \qquad (10)$$

$$E_f^2=\left(\frac{\vec{k}^2}{2m_f}+\tilde{\mu}_f\right)^2E_f=\pm\left(\frac{\vec{k}^2}{2m_f}+\tilde{\mu}_f\right). \qquad (11)$$

In the case $|\vec{k}|\ll 1$

$$E_b \approx \pm k\sqrt{\frac{\lambda_b \phi_0^{\,2}}{2m_b}}, \qquad (12)$$

associating with Goldstone bosons due to U(1) $\times$ U(1) breaking.

The CJT effective potential $V_\beta^{CJT}(\phi_0, \psi_0, D, G)$ at finite temperature in the Hartree-Fock approximation is derived

$$\begin{aligned} V_\beta^{CJT}(\phi_0, \Delta, \Delta^*, D, G) = & -\mu_b \phi_0^{\,2} + \frac{\lambda_b}{2}\phi_0^{\,4} + \frac{1}{\lambda_f}\Delta^*\Delta + \frac{1}{2}\int_\beta tr\{\ln D^{-1}(k) + [D_0^{-1}(k;\phi_0)D] - 11\} \\ & - \int_\beta tr\{\ln G^{-1}(k) + [G_0^{-1}(k;\phi_0,\Delta,\Delta^*)G] - 11\} + \frac{3\lambda_b}{8}P_{11}^{\,2} + \frac{3\lambda_b}{8}P_{22}^{\,2} + \frac{\lambda_b}{4}P_{11}P_{22} \\ & - \lambda_f Q_{11}Q_{22} + \frac{\lambda_{bf}}{4}(P_{11}+P_{22})(Q_{11}-Q_{22}), \end{aligned} \qquad (13)$$

where

$$P_{ij} = \int_\beta D_{ij}, \qquad Q_{ij} = \int_\beta G_{ij}; \qquad i, j = 1, 2.$$

The ground state in equilibrium is derived by the minimization of effective potential (13)

$$\frac{\delta V_\beta^{CJT}}{\delta \phi_0} = 0, \qquad \frac{\delta V_\beta^{CJT}}{\delta \Delta} = 0, \qquad \frac{\delta V_\beta^{CJT}}{\delta \Delta^*} = 0; \qquad (14)$$

$$\frac{\delta V_\beta^{CJT}}{\delta D} = 0, \qquad \frac{\delta V_\beta^{CJT}}{\delta G} = 0. \qquad (15)$$

(14) leads to the gap equations

$$\begin{aligned} & \phi_0(\tilde{\mu}_{b_2} + \frac{3\lambda_b}{2}P_{11} + \frac{\lambda_b}{2}P_{22} - \frac{\lambda_{bf}}{2}Q_{11} + \frac{\lambda_{bf}}{2}Q_{22}) = 0, \\ & \Delta^* = -\lambda_f Q_{21}, \\ & \Delta = -\lambda_f Q_{12}; \end{aligned} \qquad (16)$$

and (15) leads to the Schwinger-Dyson (SD) equations for propagators

$$D^{-1} = D_0^{-1} + \Sigma^\phi, \qquad (17)$$

$$G^{-1} = G_0^{-1} + \Sigma^\psi, \qquad (18)$$

in which

where

$$\Sigma_1^{\phi} = \frac{3\lambda_b}{2} P_{11} + \frac{\lambda_b}{2} P_{22} + \frac{\lambda_{bf}}{2} Q_{11} - \frac{\lambda_{bf}}{2} Q_{22}$$

$$\Sigma_2^{\phi} = \frac{\lambda_b}{2} P_{11} + \frac{3\lambda_b}{2} P_{22} + \frac{\lambda_{bf}}{2} Q_{11} - \frac{\lambda_{bf}}{2} Q_{22}$$

$$\Sigma_1^{\psi} = \lambda_f Q_{22} - \frac{\lambda_{bf}}{4} P_{11} - \frac{\lambda_{bf}}{4} P_{22} u$$

$$\Sigma_2^{\psi} = -\lambda_f Q_{11} - \frac{\lambda_{bf}}{4} P_{11} - \frac{\lambda_{bf}}{4} P_{22}. \qquad (19)$$

(18) clearly shows that the Goldstone theorem fails in the HF approximation. In order to restore it, let us invoke the method developed in [22], which in our case is achieved by adding a correction ΔV to V_β^{CJT}, namely,

$$V_\beta^{CJT} = V_\beta^{CJT} + \Delta V_\beta^{CJT} \qquad (20)$$

where

$$\Delta V_\beta^{CJT} = \frac{x\lambda_b}{2}(P_{11}^2 + P_{22}^2 - 2P_{11}P_{22}) + \frac{y\lambda_f}{2}(Q_{11}^2 + Q_{22}^2 + 2Q_{11}Q_{22}) + \frac{z\lambda_{bf}}{2}(P_{11} + P_{22})(Q_{11} - Q_{22}) \qquad (21)$$

To satisfy the Nambu-Goldstone theorem, we choose $x = -1/2$, $y = 1/2$, and $z = -1$. Then we are led to the effective potential

$$\begin{aligned}\tilde{V}_\beta^{CJT}(\phi_0, \Delta, \Delta^*, D, G) = &-\mu_b \phi_0^2 + \frac{\lambda_b}{2}\phi_0^4 + \frac{1}{\lambda_f}\Delta^*\Delta + \frac{1}{2}\int_\beta tr\left[\ln D^{-1}(k) + D_0^{-1}(k;\phi_0)D - 11\right] \\ &- \int_\beta tr\left[\ln G^{-1}(k) + G_0^{-1}(k;\phi_0,\Delta,\Delta^*)G - 11\right] \\ &+ \frac{\lambda_b}{8}P_{11}^2 + \frac{\lambda_b}{8}P_{22}^2 + \frac{3\lambda_b}{4}P_{11}P_{22} + \frac{\lambda_f}{4}Q_{11}^2 + \frac{\lambda_f}{4}Q_{22}^2 - \frac{\lambda_f}{2}Q_{11}Q_{22} \\ &- \frac{\lambda_{bf}}{4}(P_{11} + P_{22})(Q_{11} - Q_{22}), \qquad (22)\end{aligned}$$

in which

$$D^{-1} = \begin{pmatrix} \frac{\vec{k}^2}{2m_b} + \mu_b^* & -\omega_b \\ \omega_b & \frac{\vec{k}^2}{2m_b} \end{pmatrix} \tag{23}$$

$$G^{-1} = \begin{pmatrix} -i\omega_f + \frac{\vec{k}^2}{2m_f} + \mu_f^* & -\Delta \\ -\Delta^* & -i\omega_f - \frac{\vec{k}^2}{2m_f} - \mu_f^* \end{pmatrix} \tag{24}$$

with

$$\begin{aligned} \mu_b^* &= -\mu_b + 3\lambda_b\phi_0^2 + \frac{\lambda_b}{2}P_{11} + \frac{3\lambda_b}{2}P_{22} - \frac{\lambda_{bf}}{2}Q_{11} + \frac{\lambda_{bf}}{2}Q_{22}, \\ 0 &= -\mu_b + \lambda_b\phi_0^2 + \frac{3\lambda_b}{2}P_{11} + \frac{\lambda_b}{2}P_{22} - \frac{\lambda_{bf}}{2}Q_{11} + \frac{\lambda_{bf}}{2}Q_{22}, \\ \mu_f^* &= -\mu_f + \frac{\lambda_{bf}}{2}\phi_0^2 - \frac{\lambda_f}{2}Q_{11} + \frac{\lambda_f}{2}Q_{22} + \frac{\lambda_{bf}}{4}P_{11} + \frac{\lambda_{bf}}{4}P_{22}, \\ \Delta &= -\lambda_f Q_{12}, \\ \Delta^* &= -\lambda_f Q_{21}. \end{aligned} \tag{25}$$

The new effective potential obeys three requirements imposed in [22]: (i) it restores the Goldstone theorem in the broken symmetry phase, (ii) it does not change the HF equations for the mean fields and (iii) it does not change results in the phase of restored symmetry.

It is obvious that the dispersion relations received from $\det D^{-1} = 0$ and $\det G^{-1} = 0$ read

$$E_b = \sqrt{\frac{\vec{k}^2}{2m_b}\left(\frac{\vec{k}^2}{2m_b} + \mu_f^*\right)}, \tag{26}$$

$$E_f = \sqrt{\left(\frac{\vec{k}^2}{2m_f} + \mu_f^*\right)^2 + |\Delta|^2}, \tag{27}$$

expressing not only the Goldstone theorem, but also the superfluidity of condensates due to the Landau criteria [22] and, consequently, the speeds of sound in bose condensate read

$$C_b = \sqrt{\frac{\mu_b^*}{2m_b}}\ .$$

The dynamic instability takes place for bose condensate when its superfluidity is broken, that is when the corresponding speed of sound and energy become complex, namely,

$$\mu_b^* < 0. \qquad (28)$$

In studying the phase structure of bose-fermi mixture the chemical potentials have been used as the control parameters, however most experimental realizations of bose and fermi mixture in dilute atomic gases are based on systems of fixed particle numbers. Therefore in order to get an experimental relevance it is necessary to determine the total particle densities and the condensate densities of the processes considered in this work. To this end, let us begin with the pressure defined by

$$P = -\tilde{V}_\beta^{CJT}(\phi_0, \psi_0, D, G)_{\text{at minimum}} \qquad (29)$$

from which the total particle densities are derived

$$\rho_i = \frac{\partial P}{\partial \mu_i} \qquad (i = \phi \text{ or } \psi)$$

yielding

$$\begin{aligned} \rho_b &= \phi_0^2 + \frac{1}{2}(P_{11} + P_{22}) \\ \rho_f &= -Q_{11} + Q_{22}, \end{aligned} \qquad (30)$$

and

$$\begin{aligned} \mu_b^* &= -\mu_b + 3\lambda_b\rho_b + \frac{\lambda_{bf}}{2}\rho_f - \lambda_b P_{11}, \\ 0 &= -\mu_b + \lambda_b\rho_b + \frac{\lambda_{bf}}{2}\rho_f + \lambda_b P_{11}, \\ \mu_b^* &= -\mu_f + \frac{\lambda_f}{2}\rho_f + \frac{\lambda_{bf}}{2}\rho_b, \\ \Delta &= -\lambda_f Q_{12}, \\ \Delta^* &= -\lambda_f Q_{21}. \end{aligned}$$

Inserting (30) into (29) lead to

$$P = \frac{\lambda_b}{2}\rho_b^2 + \frac{\lambda_f}{4}\rho_f^2 + \frac{\lambda_{bf}}{2}\rho_b\rho_f - \frac{1}{\lambda_f}\Delta^*\Delta$$

$$- \frac{1}{2}\int_\beta tr \ln D^{-1}(k) + \int_\beta tr \ln G^{-1}(k) + \lambda_b\rho_b P_{11} - \frac{\lambda_b}{2}P_{11}^2. \qquad (32)$$

Eq. (32) constitute the EoS governing all thermodynamical processes, in particular, phase transitions of the binary mixture, which is a two-component system with two conserved charges.

In the following the formulae (22), (29), (30) and (32) will be widely employed in the numerical study of dynamical stability and phase structure of bose-fermi mixtures.

3. Numerical study

The main aim of this Section is to explore the phase transitions and their related phase structures based on the phase diagram in the (T, μ)-plane. Then making use of this phase diagram we will prove that the binary bose-fermi mixture is featured by the following properties:

1. Depending on the dynamical stability of the system we could observe one of the phases $(\phi_0 \neq 0, |\Delta| = 0)$, $(\phi_0 = 0, |\Delta| \neq 0)$, $(\phi_0 \neq 0, |\Delta| \neq 0)$ and a desert $(\phi_0 = 0, |\Delta| = 0)$.

2. Where the dynamical stability be present, $M_b > 0$, there the corresponding order parameter acquires a non-vanishing value, $\phi_0 \neq 0$, therefore the corresponding symmetry U(1) is spontaneously broken, and there exists a condenstate of bose gas.

3. The evolution of specific heat at constant volume C_V versus T (or μ) allows us to assert which scenario possibly exists in nature.

We use values of the parameters for ^{40}K-^{87}Rb and ^{6}Li-^{87}Rb mixtures as given in Table 1.

Table 1: List of parameters of the experiments with ^{40}K-^{87}Rb and ^{6}Li-^{87}Rb boson-fermion mixture. The values are taken from [35]−[38].

Parameters	^{40}K−^{87}Rb	^{6}Li−^{87}Rb
Mass ratio m_f/m_b	0.46	0.08
s-wave scattering length (bosons−bosons)	99 a_0	
s-wave scattering length (fermions−fermions)	174 a_0	
s-wave scattering length (bosons−fermions)	$\pm$ 284 a_0	
fermion energy	$k_B \times 1.5\mu$K	$k_B \times 5\mu$K

The numerical computation performed in the Appendix yields the self-enersies. The phase diagrams for repulsive $(a_{BF} > 0)$ and attractive $(a_{BF} < 0)$ Bose-Fermi interactions are shown in Fig.1 as a function of the boson and fermion chemical potentials. In both cases, a qualitatively similar structure emerges:

The transition between the pure fermion and the phase where boson and fermions form a homogeneous mixture (mixed phase) is first order (thick solid red line). On the other hand, the transition between the pure boson and the mixed phases (thin solid black line) is second order, i.e. continuous. This transition coincides with the locus of points where the system first develops a Fermi surface, i.e., $\mu_f^* - \mathrm{sign}(\lambda_{bf})\rho_b = 0$, and therefore $\mu_f > 0$ ($\mu_f < 0$) for repulsive (attractive) interactions. Finally, the transitions between the vacuum, corresponding to zero density of both fermions and bosons, and either the pure boson or fermion phases (thin solid black lines in Fig.1) are continuous, as they correspond to the filling of a band. Therefore, the first order line separating the pure fermion and mixed phases te rminates at the origin $(\mu_f, \mu_b) = (0,0)$ in a tricritical point (filled blue circle), where the first order transition becomes second order.

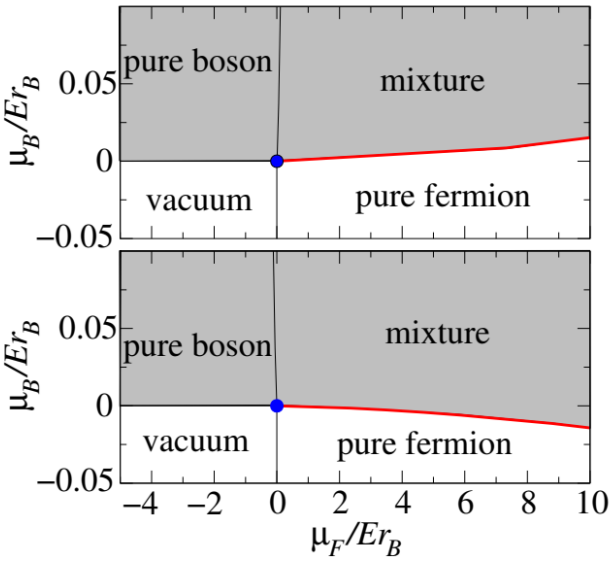

Figure 1: (Color online) Zero temperature phase diagrams for a \emph{repulsive} ($a_{bf} > 0$, top panel) and \emph{attractive} $a_{bf} < 0$ (bottom panel) Bose-Fermi mixture where $E r_B$ is the boson recoil energy. The thin solid black lines correspond to 2nd order (i.e. continuous) phase transitions between either the vacuum and the pure boson/fermion phases or between the pure boson and the homogeneous mixed phase. The thick solid (red) line corresponds to a first order transition between the pure fermion and the mixed phase. Second and first order lines meet at at the tricritical point at $\mu_f = \mu_b = 0$ (filled blue circle). The region with finite boson density is the light gray shaded region. In both cases phase separation can only occur between a mixed and pure fermion phases.

A first order transition in the phase diagram in chemical potential space implies that the system exhibits phase separation in density space, where, rather than fixing the chemical potentials μ_f and μ_b, one fixes the boson and fermion densities (see Fig.2). We obtain therefore that phase separation is only possible between pure fermion and mixed phases (dot-dashed black lines in Fig.2). This result, by the non-perturbative treatment of the boson interactions employed here, yields a first order transition between the pure fermion and mixed phases.

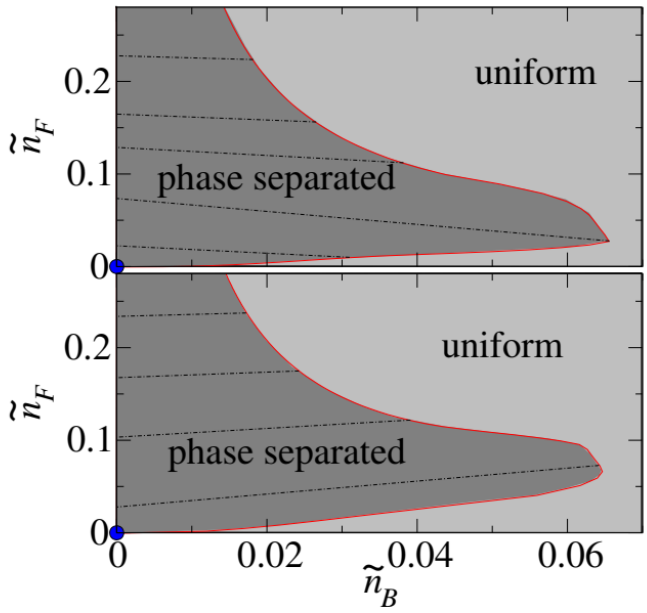

Figure 2: (Color online) Phase diagrams in the density plane $(\tilde{n}_B, \tilde{n}_F)$. The corresponding phase diagrams in the chemical potential plane (not shown for brevity) display the same features and phase topology as the diagrams shown Fig.1 but for which the phase boundary in the density plane proved much harder to determine numerically. The top panel corresponds to a repulsive Bose-Fermi interactions, whereas in the bottom corresponds to attractive interactions. In both cases, the system can either be in a uniform mixed phase (lightly gray shaded region) or, by undergoing a first order transition, it can be in a phase separated state (dark gray shaded region), where a pure fermion and mixed phase coexist. The dot-dashed lines connect points on the first order boundary with the same values of the chemical potentials.

Now let us discuss the numerical solutions of Eq. (29) obtained by using a stabilized iterative procedure. Since the function Δ has an axial symmetry, it suffices to consider a cross section of its energy gap at $k_y = 0$. Figure 3 presents typical examples of this cross section at fixed temperature. It is seen from Fig. 3 that the maximum of the energy gap is localized near the points $(0, 0, \pm k_F)$, and the maximal energy gap monotonically decreases as temperature increases ([see the inset in Fig. 3 and Fig. 4. The energy gap in the *p*-phase vanishes at some critical temperature T_c. The energy gap is a function of interaction constants and densities of the Bose- and Fermi-gases. Figure 5 illustrates how the energy gap is affected by variation of the Bose-gas density.

The non-trivial dependence of the maximal gap Δ_p on k_F^{-1}, at $T = 0$ comes from the Bogolyubov dispersion relations (26) and (27) of the Bose gas. Such a dependence should be taken into account in the experimental observation of the *p*-wave superfluid state.

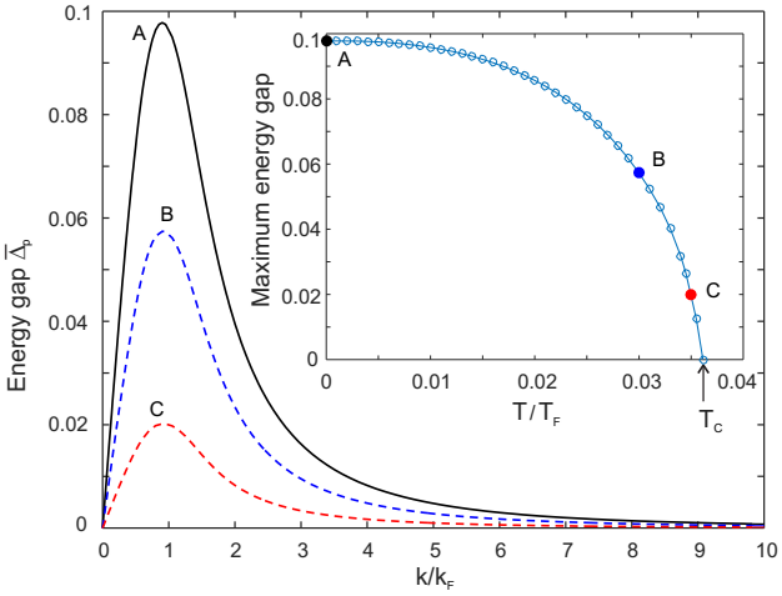

Figure 3: Typical examples of the energy gap Δ in the *p*-wave polar phase found numerically at different temperatures (A: $T = 0$, B: $T = 0.03T_F$, and C: $T = 0.035T_F$). The inset presents the maximum of the energy gap as a function of temperature. Note that the energy gap vanishes at the critical temperature T_c.

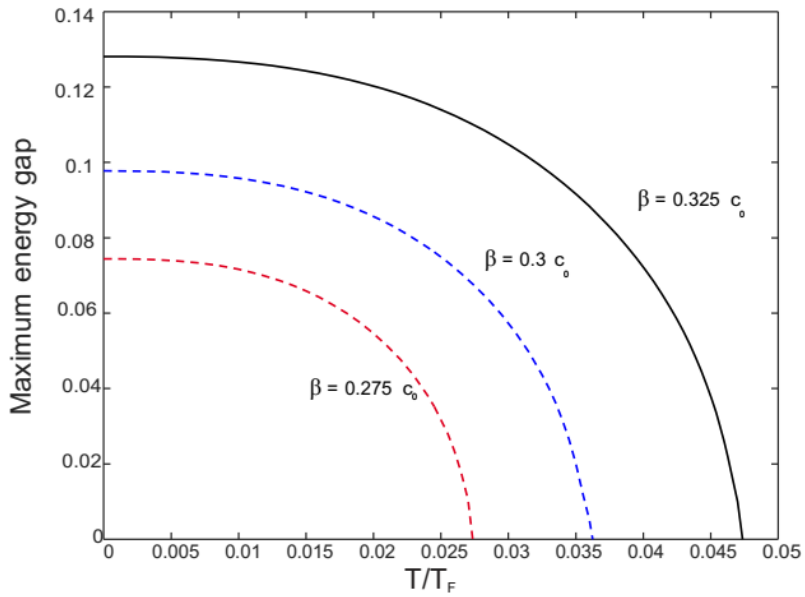

Figure 4: The maximal energy gap as a function of temperature for different values of β indicated near the curves. The concentrations of bosons and fermions are fixed as follows: $n_B = n_F = 10^{14} cm^{-3}$.

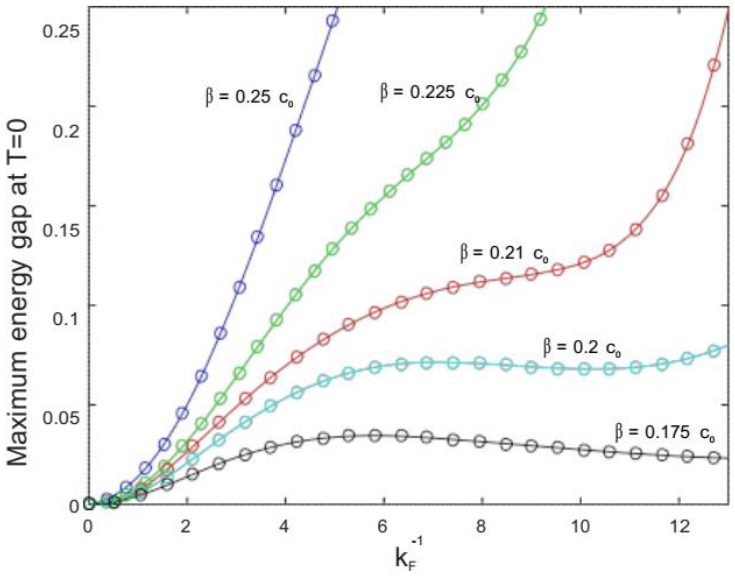

Figure 5: The maximal energy gap at $T = 0$ as a function of k_F^{-1} at $n_F = 10^{14}$ cm^{-3} is plotted for different values of β.

4. Conclusion and discussion

A effective action framework for describing binary atomic Bose-Fermi mixtures has been presented here. By entering integrations of the bosons and fermions in the effective action and using the two-loop expansion to find the effective potential of the composite system, the nature of the mixture - phase separation transition can be visualized clearly as the free-energy curve intersects itself. The construction of phase separation is complicated by the compressibility of atomic gases, which differentiate this work from conventional liquid or solid mixtures. The phase diagrams presented here guarantees mechanical and diffusive equilibrium because the lever rule has been implemented. The framework is versatile and applicable to other binary atomic mixtures.

We showed that a mixture of dilute ultracold bosonic and fermionic atoms provides a promising platform for the realization of the *p*-wave superfluid state. We derived a general set of the gap equations for the energy gaps in the *s*- and *p*-channels and the SD equations for the bosonic and fermionic propagators. It is found that the spin-induced interactions in a mixture of bosonic and fermionic atoms naturally suppress the s-wave pairing. At the same time the p-wave pairing is driven not only by density-induced interaction, but also by spin-induced interactions and it emerges even for repulsive interaction between fermions. While the dependence of the maximal value of the gap on temperature is a monotonically decreasing function, its dependence on the density of bosons n_B is non-monotonous for sufficiently small values of the spin-spin bose-fermi interaction β. Such a dependence comes from the corresponding non-trivial dependence of the Bogolyubov dispersion relations on n_B.

We hope that the results presented in this paper will stimulate experiments to observe the *p*-wave superfluid in a mixture of ultracold Fermi and spinor Bose gases. Moreover, the study of the *p*-wave superfluidity in a wellcontrolled environment of atomic physics could help to elucidate the properties of topologically non-trivial superfluids.

Therefore, while the theory presented here offers an overview of binary atomic Bose-Fermi mixtures and captures the main features, future investigations with more complicated treatments will further improve the theoretical framework.

Acknowledgments. This paper is supported by the Vietnam Ministry of Education and Training in the framework of the Scientific Research Project under Grant B 2015-25-33.

Appendix

Using

$$\sum_{n=-\infty}^{\infty} \frac{1}{\omega_b^2 + E^2} = \frac{1}{2ET}\left(1 + \frac{2}{e^{E/T} - 1}\right); \quad \omega_b = 2n\pi T;$$

$$\sum_{n=-\infty}^{\infty} \ln\left(\omega_b^2 + E^2\right) = \frac{E}{T} + 2\ln\left(1 - e^{-E/T}\right); \sum_{n=-\infty}^{\infty} \frac{-1}{i\omega_f - E^+} = \frac{1}{2T}(1 - \frac{2}{e^{E^+/T} + 1}); \quad \omega_f = (2n+1)\pi T;$$

$$\sum_{n=-\infty}^{\infty} \frac{-1}{i\omega_f - E^-} = \frac{1}{2T}(-1 + \frac{2}{e^{E^-/T} + 1});$$

$$\sum_{n=-\infty}^{\infty} \ln\left(i\omega_f - E^+\right) = \frac{E^+}{2T} + \ln\left(1 + e^{-E^+/T}\right);$$

$$\sum_{n=-\infty}^{\infty} \ln\left(i\omega_f - E^-\right) = -\frac{E^-}{2T} + \ln\left(1 + e^{E^-/T}\right);$$

$$\sum_{-\infty}^{\infty} \frac{1}{(i\omega_f - E\wedge+)(i\omega_f - E\wedge-)} = \frac{1}{(E^+ - E^-)T}(\frac{1}{e^{E^+/T} + 1} + \frac{1}{e^{-E^-/T} + 1} - 1),$$

and dimensional regularization integral with $d = 3 - 2^{\epsilon}$

$$I_{m,n}(M) = \int \frac{d^d p}{(2\pi)^d} \frac{p^{2m}}{(p^2 + M)^n} = \frac{M^{d/2+m-n}}{(4\pi)^{d/2}} \frac{\Gamma\left(n - m - d/2\right)\Gamma\left(d/2 + m\right)}{\Gamma\left(d/2\right)\Gamma\left(n\right)},$$

for bosons we get with ($p^2 = k^2/2m$)

$$\frac{1}{2}\int_\beta tr\ln D^{-1}(k) = \frac{(2m_\phi)^{3/2}}{30\pi^2}M_\phi^{5/2} + (2m_\phi)^{3/2} I_3^\phi[M_\phi, T],$$

$$P_{11} = \frac{(2m_\phi)^{3/2}}{6\pi^2}M_\phi^{3/2} + (2m_\phi)^{3/2} I_1^\phi[M_\phi, T],$$

$$P_{22} = -\frac{(2m_\phi)^{3/2}}{12\pi^2}M_\phi^{3/2} + (2m_\phi)^{3/2} I_2^\phi[M_\phi, T],$$

and dimensional regularization integral

$$I_{m,n}(M,\Delta) = \int \frac{d^d p}{(2\pi)^d}\frac{p^{4m}}{[(p^2+M)^2+\Delta^2]^n}$$
$$= \frac{\Delta^{d/2+2m-2n}}{(4\pi)^{d/2}}\frac{\Gamma(n-m-d/4)\Gamma(m+d/4)}{2\Gamma(d/2)\Gamma(n)} \times {}_2F_1(d/4-m, n-m-d/4; d/2; -M^2/\Delta^2),$$

for femions we get with ($p^2 = k^2/2m$)

$$\int_\beta \mathrm{tr}\ln G^{-1}(k) = -\frac{(2m_\psi)^{3/2}}{5\pi^{5/2}}\Gamma^2(3/4)|\Delta|^{5/2}\ {}_2F_1\left(-\frac{5}{4}, \frac{3}{4}; \frac{3}{2}; -\frac{M_\psi^{*2}}{|\Delta|^2}\right) + (2m_\psi)^{3/2} I_3^\psi[M_\psi^*, T],$$

$$Q_{11} = -\frac{(2m_\psi)^{3/2}|\Delta|^{1/2}}{4\pi^{5/2}}\left[\frac{|\Delta|\Gamma^2(1/4)}{12}\ {}_2F_1\left(-\frac{3}{4}, \frac{1}{4}; \frac{3}{2}; -\frac{M_\psi^{*2}}{|\Delta|^2}\right) + M_\psi^*\Gamma^2(3/4)\ {}_2F_1\left(-\frac{1}{4}, \frac{3}{4}; \frac{3}{2}; -\frac{M_\psi^{*2}}{|\Delta|^2}\right)\right] - \frac{(2m_\psi)^{3/2}}{2} I_2^\psi[M_\psi^* T],$$

$$Q_{22} = \frac{(2m_\psi)^{3/2}|\Delta|^{1/2}}{4\pi^{5/2}}\left[\frac{|\Delta|\Gamma^2(1/4)}{12}\ {}_2F_1\left(-\frac{3}{4}, \frac{1}{4}; \frac{3}{2}; -\frac{M_\psi^{*2}}{|\Delta|^2}\right) + M_\psi^*\Gamma^2(3/4)\ {}_2F_1\left(-\frac{1}{4}, \frac{3}{4}; \frac{3}{2}; -\frac{M_\psi^{*2}}{|\Delta|^2}\right)\right] + \frac{(2m_\psi)^{3/2}}{2} I_2^\psi[M_\psi^* T],$$

$$Q_{12} = \frac{(2m_\psi)^{3/2}\Delta}{4\pi^{5/2}}|\Delta|^{1/2}\ \Gamma^2(3/4)\ {}_2F_1(-1/4, 3/4; 3/2; -M_\psi^{*2}/|\Delta|^2) + \frac{(2m_\psi)^{3/2}\Delta}{2} J^\psi[M_\psi^*, T],$$

$$Q_{21} = \frac{(2m_\psi)^{3/2}\Delta}{4\pi^{5/2}}|\Delta|^{1/2}\ \Gamma^2(3/4)\ {}_2F_1(-1/4, 3/4; 3/2; -M_\psi^{*2}/|\Delta|^2) + \frac{(2m_\psi)^{3/2}\Delta^*}{2} J^\psi[M_\psi^*, T],$$

where

$$I_1^\phi[M_\phi, T] = \int_0^\infty \frac{dp}{2\pi^2}\frac{p^3}{\sqrt{p^2+M_\phi}}\frac{1}{e^{p\sqrt{p^2+M_\phi}/T}-1},$$

$$I_2^\phi[M_\phi, T] = \int_0^\infty \frac{dp}{2\pi^2}\frac{p\sqrt{p^2+M_\phi}}{e^{p\sqrt{p^2+M_\phi}/T}-1},$$

$$I_3^\phi[M_\phi, T] = T\int_0^\infty \frac{p^2 dp}{2\pi^2}\ln\left(1-e^{-p\sqrt{p^2+M_\phi}/T}\right),$$

$$I_2^{\psi}[M_{\psi},T] = \int \frac{dp}{2\pi^2} \frac{p^2(p^2+M_{\psi})}{\sqrt{(p^2+M_{\psi})^2+|\Delta|^2}} \left(\frac{1}{e^{E_{\psi}^{+}/T}+1} + \frac{1}{e^{-E_{\psi}^{-}/T}+1} \right),$$

$$I_3^{\psi}[M_{\psi},T] = T \int \frac{p^2 dp}{2\pi^2} \left[\ln\left(1+e^{-E_{\psi}^{+}/T}\right) + \ln\left(1+e^{E_{\psi}^{-}/T}\right) \right],$$

$$J^{\psi}[M_{\psi},T] = \int \frac{d^3p}{(2\pi)^3} \frac{1}{\sqrt{(p^2+M_{\psi})^2+|\Delta|^2}} \left(\frac{1}{e^{E_{\psi}^{+}/T}+1} + \frac{1}{e^{-E_{\psi}^{-}/T}+1} \right).$$

REFERENCES

[1] C. J. Myatt et al., (1997), Phys. Rev. Lett. 78, 586

[2] D. S. Hall et al., (1998), Phys. Rev. Lett. 81, 1539

[3] D. M. Stamper-Kurn et al., (1999), Phys. Rev. Lett. 83, 661

[4] M. R. Matthews et al.,(1999), Phys. Rev. Lett. 83, 2498

[5] H. J. Miesner et al.,(1999), Phys. Rev. Lett. 82, 2228

[6] D. J. McCarron et al., (2011), Phys. Rev. A 84, 011603(R)

[7] S. B. Papp, J. M. Pino and C. E. Wieman, (2008), Phys. Rev. Lett. 101, 040402

[8] C. J. Pethick and H. Smith, (2002), Bose-Einstein condensation in dilute gases (Cambridge University Press.

[9] F. Schreck, L. Khaykovich, K. L. Corwin, G. Ferrari, T. Bourdel, J. Cubizolles, and C. Salomon, (2001), Phys. Rev. Lett. 87, 080403

[10] A. G. Truscott, K. E. Strecker, W. I. McAlexander, G. B. Partridge, and R. G. Hulet, (2001), Science 291, 2570

[11] G. Roati, F. Riboli, G. Modugno, and M. Inguscio, (2002), Phys. Rev. Lett. 89, 150403

[12] B. Deh, C. Marzok, C. Zimmermann, and P. W. Courteille, (2008), Phys. Rev. A 77, 010701

[13] M. K. Tey, S. Stellmer, R. Grimm, and F. Schreck, (2010), Phys. Rev. A 82, 011608

[14] X.-C. Yao, H.-Z. Chen, Y.-P. Wu, X.-P. Liu, X.-Q. Wang, X. Jiang, Y. Deng, Y.-A. Chen, and J.-W. Pan, (2016), Phys. Rev. Lett. 117, 145301

[15] R. S. Lous, I. Fritsche, M. Jag, F. Lehman, E. Kirilov, B. Huang, and R. Grimm (2018), arXiv: 1802.01954.

[16] B. J. DeSalvo, K. Patel, J. Johansen, and C. Chin, (2017), Phys. Rev. Lett. 119, 233401

[17] K. Mølmer, Phys. Rev. Lett. 80, 1804 (1998); L. Viverit, C.J. Pethick, H. Smith, (2000), Phys. Rev. A 61, 053605

[18] G. Modugno, G. Roati, F. Riboli, F. Ferlaino, R.J. Brecha, M. Inguscio, (2002), Science 297, 2240

[19] C. Ospelkaus, S. Ospelkaus, K. Sengstock, K. Bongs, (2006), Phys. Rev. Lett. 96, 020401

[20] F. M. Marchetti, C. Mathy, M. M. Parish, D. A. Huse, (2008), Phys. Rev. B 78, 134517

[21] A. Simoni, F. Ferlaino, G. Roati, G. Modugno, M. Inguscio, Phys. Rev. Lett. 90, 163202 (2003); C. A. Stan, M. W. Zwierlein, C.H. Schunck, S.M.F. Raupach, W. Ketterle, Phys. Rev. Lett. 93, 143001 (2004); S. Inouye, J. Goldwin, M. L. Olsen, C. Ticknor, J. L. Bohn, D. S. Jin, Phys. Rev. Lett. 93, 183201 (2004); F. Ferlaino, C. D'Errico, G. Roati, M. Zaccanti, M. Inguscio, G. Modugno, A. Simoni, Phys. Rev. A 73, 40702 (2006); M. Zaccanti, C. D'Errico, F. Ferlaino, G. Roati, M. Inguscio, G. Modugno, Phys. Rev. A 74, 041605 (2006); S. Ospelkaus, C. Ospelkaus, L. Humbert, K. Sengstock, K. Bongs, Phys. Rev. Lett. 97, 120403

[22] T. H. Phat, L. V. Hoa, Nguyen Tuan Anh, N. V. Long, Ann, (2009), Phys. (NY) 324, 2074

[23] T. H. Phat, Nguyen Tuan Anh, L. V. Hoa, D. T. M. Hue, Int. J. Mod, (2016), Phys. B 30, 1650195

[24] J. M. Cornwall, R. Jackiw and E. Tomboulis, (1974), Phys. Rev. D 10, 2428

[25] G. Amelia-Camelia, Nucl. Phys. B 476, 255 (1996); G. Amelia-Camelia and S. Y. Pi, (1993), Phys. Rev. D 47, 2356

[26] Tran Huu Phat, Le Viet Hoa, Nguyen Tuan Anh, and Nguyen Van Long (2007), Phys. Rev. D 76, 125027

[27] Tran Huu Phat, Nguyen Van Long, Nguyen Tuan Anh, and Le Viet Hoa, (2008), Phys. Rev. D 78, 105016

[28] Tran Huu Phat, Nguyen Tuan Anh, Nguyen Van Long, and Le Viet Hoa (2007), Phys. Rev. C 76, 045202

[29] Tran Huu Phat, Nguyen Tuan Anh, and Nguyen Van Long, (2008), Phys. Rev. C 77, 054321

[30] I. Ferrier-Barbut, M. Delehaye, S. Laurent, A. T. Grier, M. Pierce, B. S. Rem, F. Chevy, and C. Salomon, (2014), Science 345, 1035

[31] R. Roy, A. Green, R. Bowler, and S. Gupta, (2017), Phys. Rev. Lett. 118, 055301

[32] D. S. Hall, M. R. Matthews, J. R. Ensher, C. E. Wieman, and E. A. Cornell, (1998), Phys. Rev. Lett. 81, 1539

[33] X. Cui and T.-L. Ho, (2013), Phys. Rev. Lett. 110, 165302

[34] G.-B. Jo, Y.-R. Lee, J.-H. Choi, C. A. Christensen, T. H. Kim, J. H. Thywissen, D. E. Pritchard, and W. Ketterle, (2009), Science 325, 1521

[35] C. Ospelkaus, S. Ospelkaus, K. Sengstock, K. Bongs, (2006), Phys. Rev. Lett. 96, 020401

[36] C-H. Wu, I. Santiago, J. W. Park, P. Ahmadi, M. W. Zwierlein, (2011), Phys. Rev. A 84, 011601(R)

[37] O.Y. Matsyshyn, A.I. Yakimenko, E.V. Gorbar, S.I. Vilchinskii, V.V. Cheianov, (2018), arXiv:1803.06709

[38] T. Kim, C-C. Chien, (2018), Phys. Rev. A 97, 033628

CẤU TRÚC PHA CỦA HỖN HỢP NGUYÊN TỬ HAI THÀNH PHẦN BOSE-FERMI Ở NHIỆT ĐỘ XÁC ĐỊNH

Nguyễn Tuấn Anh[1], Đinh Thanh Tâm[2]
[1]Trường Đại học Điện Lực
[2]Trường Đại học Tây Bắc

Tóm tắt: *Nhiều các phát hiện thực nghiệm về hỗn hợp nguyên tử hai thành phần Bose-Fermi đã tạo cơ hội cho việc nghiên cứu các hệ lượng tử phức hợp với các số liệu thống kê spin khác nhau. Các hỗn hợp nguyên tử hai thành phần có thể thể hiện sự chuyển đổi cấu trúc từ hỗn hợp sang pha chia tách khi tương tác boson-fermion tăng lên. Sử dụng hình thức luận Cornwall-Jackiw-Tomboulis để tính hàm phân bố lớn và thế nhiệt động lực học, chúng tôi thu được thế hiệu dụng của hỗn hợp hai thành phần Bose-Fermi. Các đại lượng nhiệt động lực học trong một phạm vi rộng của nhiệt độ và tương tác cũng được rút ra. Quá trình chuyển đổi cấu trúc có thể được xác định là một vòng lặp của đường cong thế hiệu dụng và phần thể tích của pha chia tách có thể được xác định theo quy tắc đòn bảy. Đối với* $^{40}\mathrm{K}-^{87}\mathrm{Rb}$ *và hỗn hợp* $^{6}\mathrm{Li}-^{87}\mathrm{Rb}$*, chúng tôi biểu diễn các giản đồ pha của hỗn hợp tại nhiệt độ 0 và nhiệt độ hữu hạn.*